

Matter, Volume 3

Supplemental Information

Enhanced Bulk Transport in Copper Vanadate

Photoanodes Identified by Combinatorial Alloying

Paul F. Newhouse, Dan Guevarra, Lan Zhou, Yu Wang, Mitsutaro Umehara, David A. Boyd, John M. Gregoire, and Joel A. Haber

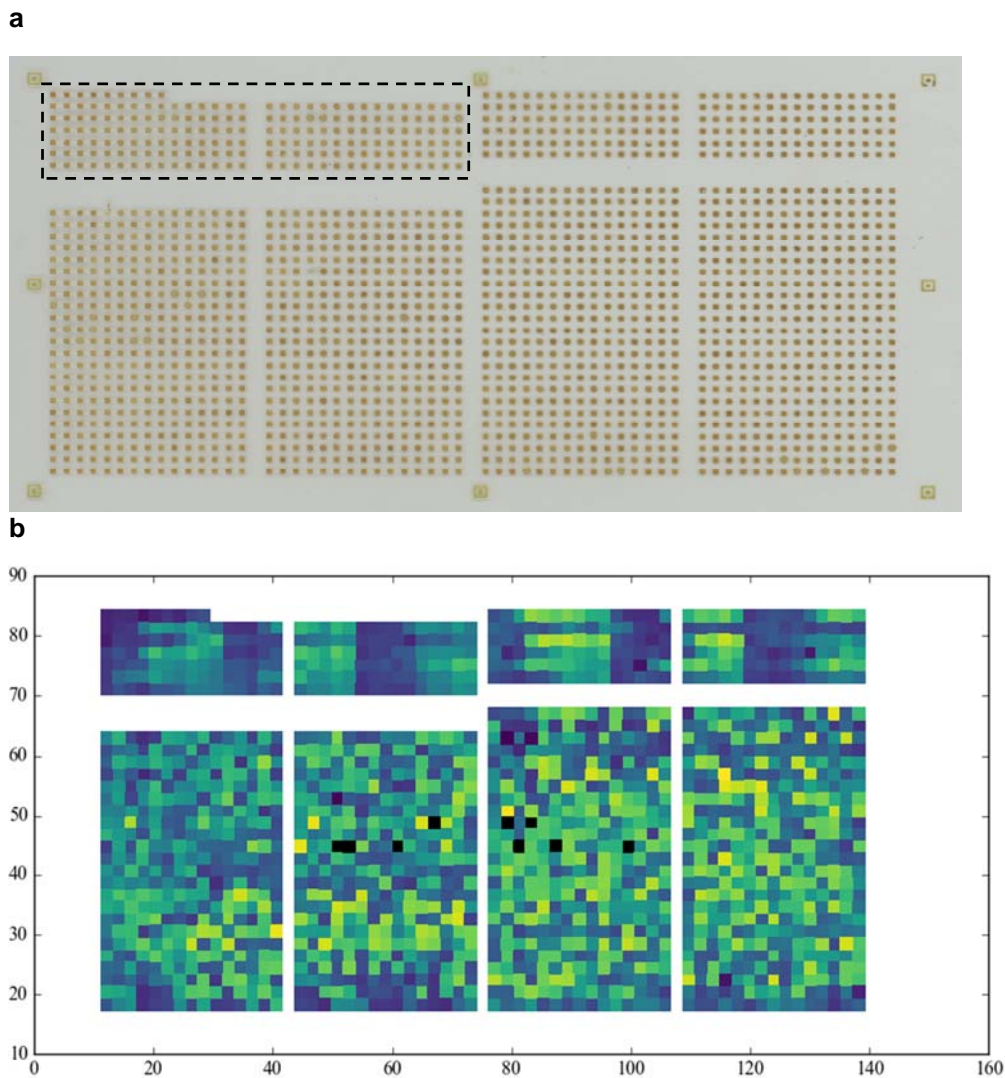


Figure S1(a), related to Figure 1. Full plate image of a $\text{Cu}_2\text{V}_2\text{O}_7$ alloy library. The substrate dimensions are 150 mm x 100 mm and each sample is ~ 1 mm x 1 mm. The systematically arranged, single element alloy composition samples are at the top of the plate, above the break. The samples shown in Fig. 1 are contained within the dashed-line rectangle. Samples are not systematically arranged according to composition below the break to avoid convolution of composition with spatial effects from synthesis or measurement. Eight fiducial markers can also be seen. **(b)** The measured figure of merit value (SLF9 P_{\max}) plotted as a color-scale on each sample location (samples in black are off-scale measurement artifacts). The trends in performance as a function of composition are apparent in the top portion of the plate, while no spatial trends are apparent in the non-systematically arranged compositions below the break.

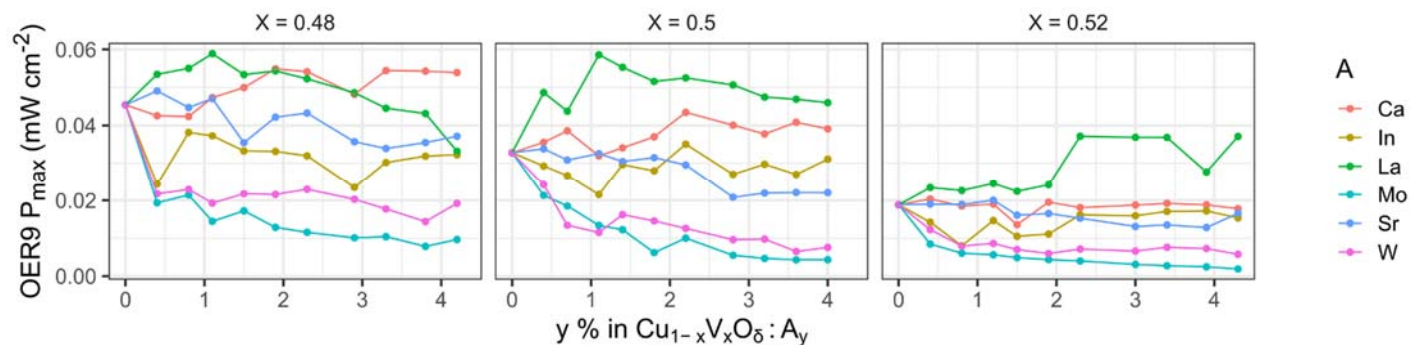


Figure S2, related to Results and Discussion section. OER9 P_{max} versus alloy loading from a $\text{Cu}_2\text{V}_2\text{O}_7$ -based library containing Mo and W, which are shown to exhibit a deleterious effect on PEC performance and were therefore excluded from more thorough investigation.

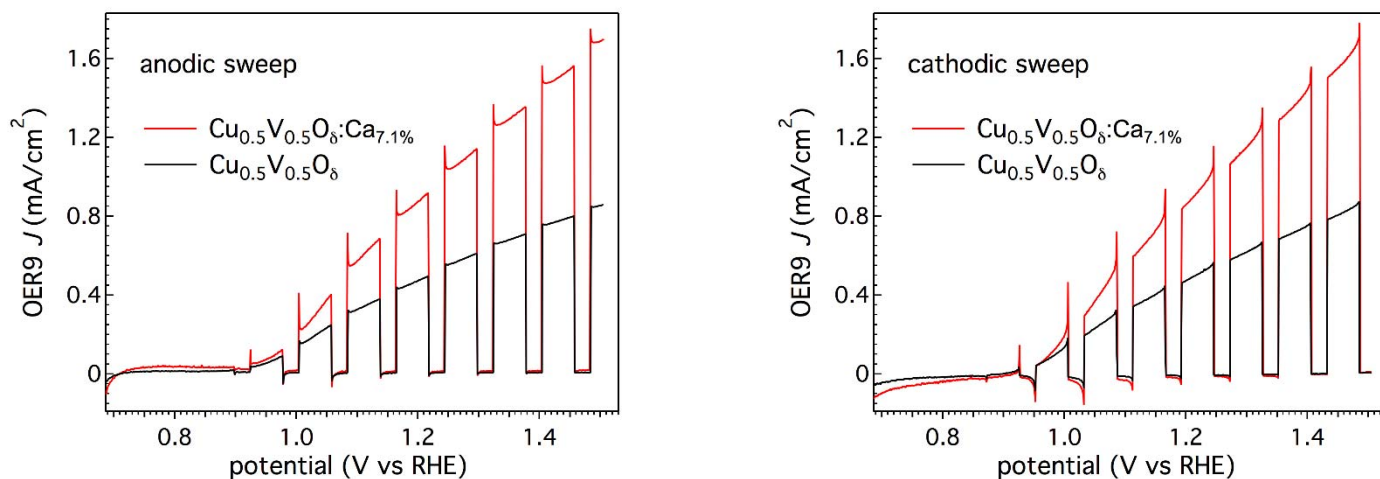


Figure S3, related to Figure 2a. OER9 (a) anodic and (b) cathodic CV sweeps from a $\text{Cu}_{0.5}\text{V}_{0.5}\text{O}_{5-delta}:\text{Ca}_{7.1\%}$ single alloy high performing sample.

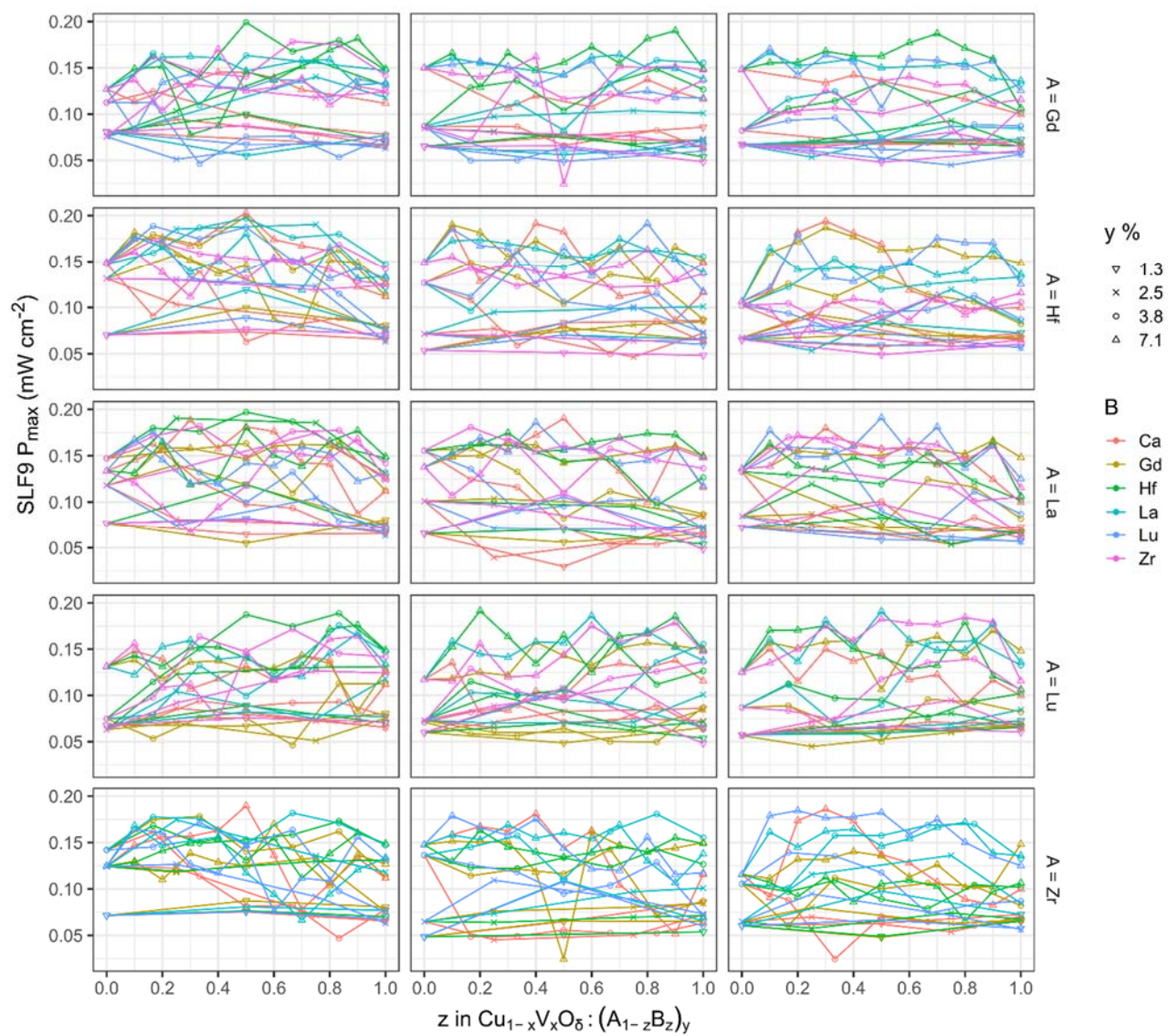


Figure S4, related to Figure 2b and Figure 3. SLF9 P_{max} vs. co-alloy fraction from samples not shown in Figs. 2b & 3.

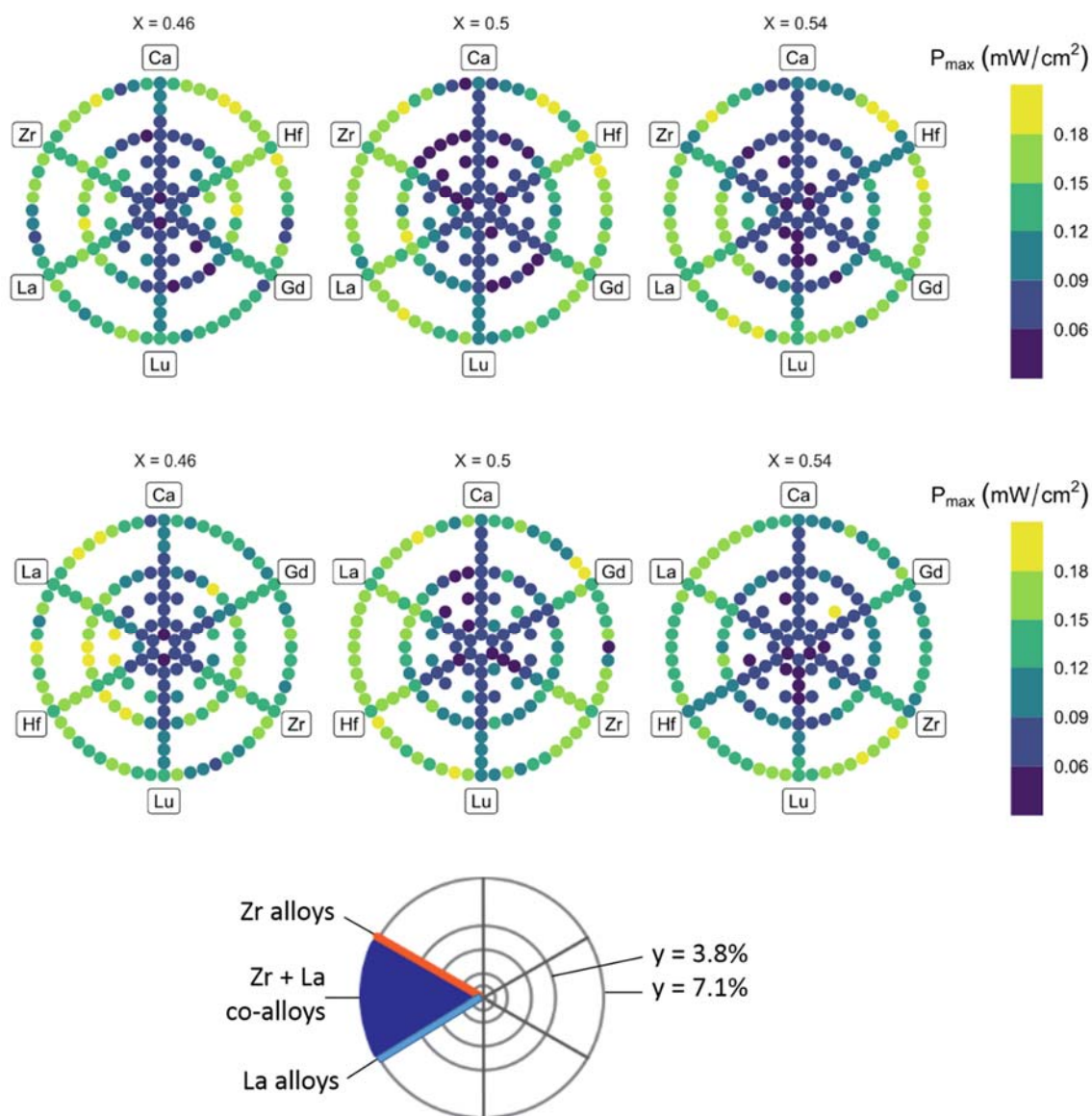


Figure S5, related to Figure 2b and Figure 3. Alternative custom visualization with alloy compositions arranged in a wheel and spoke arrangement, selected to include the highest performing co-alloy samples. The center of the center of the circle represents the 0% alloying element added, the radial spokes represent increasing concentrations of a single alloying element (six spokes for each of the alloying elements) and the circles represent co-alloying compositions with the arc connecting the spokes representing varying amounts of the two alloying elements of the connected spokes. A new plot is required for each $V/(Cu+V)$ mole ratio. In order to visualize Ca-B co-alloying performance three different plots would be required (to visualize all possible combinations of co-alloying elements would require 15 plots times 3 different $V/(Cu+V)$ ratio—to many plots for ready comprehension).

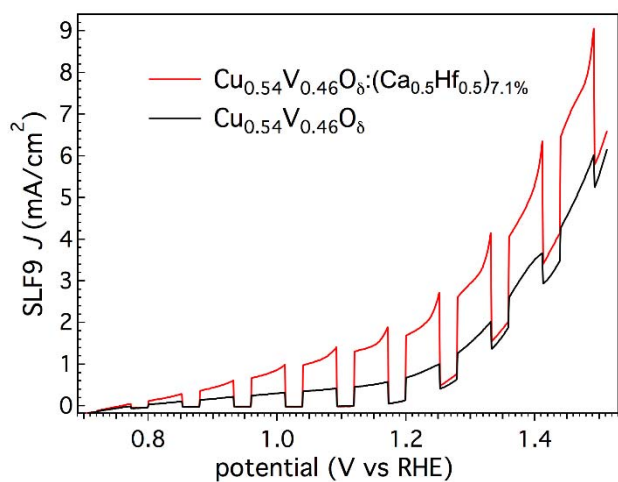


Figure S6, related to Figure 3 and Figure 4. SLF9 cathodic CV sweep from the Ca-Hf co-alloyed champion.

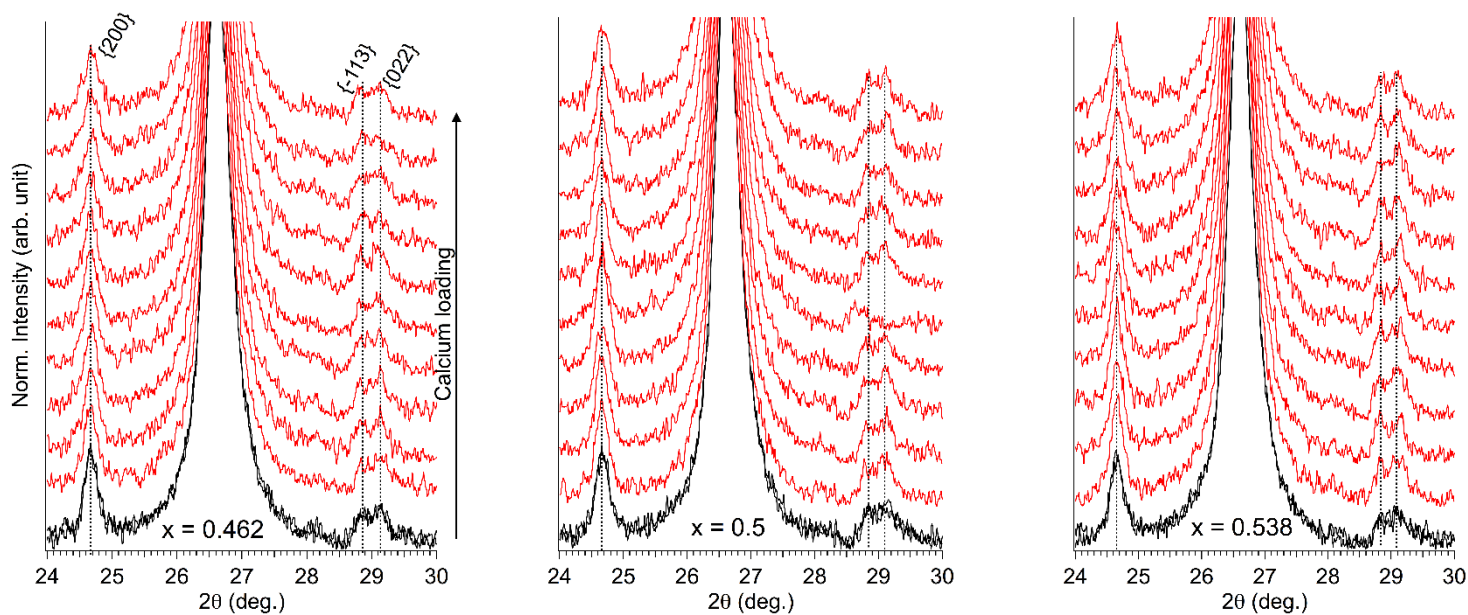


Figure S7, related to Structural characterization section. XRD spectra of $\text{Cu}_{1-x}\text{V}_x\text{O}:\text{Ca}_y$ alloys.

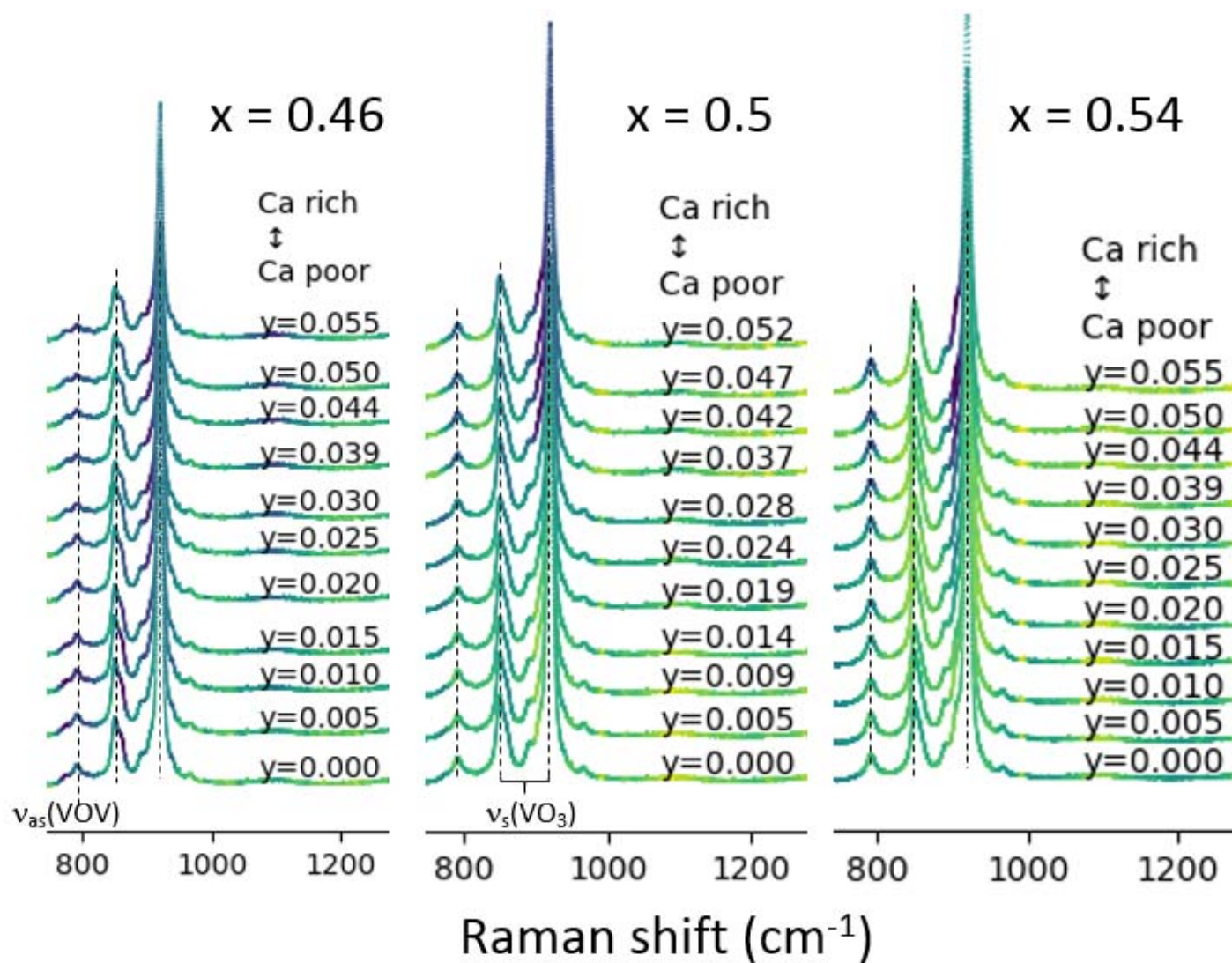


Figure S8, related to Structural characterization section. Raman patterns for all samples of composition $\text{Cu}_{1-x}\text{V}_x\text{O}:\text{Ca}_y$. Each spectrum is an average of 5 composition duplicates. Slight differences in peak shape with host composition and increased alloying can be observed for $x = 0.46$ compared to $x = 0.5$ and 0.54 .

icdd PDF #	Formula unit	crystal system	space group	a (Å)	b (Å)	c (Å)	α (deg.)	β (deg.)	γ (deg.)	vol. (Å ³)	vol. per cation (Å ³)	V at. %	Cu at. %
04-011-1618	Cu ₅ V ₂ O ₁₀	monoclinic	p21/N(14)	15.72	6.07	8.39	90.0	102.4	90.0	781.8	27.9	0.29	0.71
04-012-8670	Cu ₁₁ V ₆ O ₂₆	triclinic	P-1(2)	8.16	8.27	8.04	107.1	91.4	106.4	493.8	29.0	0.35	0.65
04-010-1734	Cu ₃ V ₂ O ₈	triclinic	P-1(2)	5.36	6.51	5.20	91.3	111.9	69.2	155.7	31.1	0.4	0.6
04-013-2998	Cu ₃ V ₂ O ₈	monoclinic	P21/a(14)	6.38	7.99	6.25	90.0	111.5	90.0	296.4	29.6	0.4	0.6
00-044-1480	Cu ₃ V ₂ O ₈	triclinic	P-1(2)	5.36	6.54	5.20	91.4	112.0	69.2	156.7	31.3	0.4	0.6
04-013-2111	Cu ₂ V ₂ O ₇	orthorhombic	Fdd2(43)	8.39	20.68	6.45	90.0	90.0	90.0	1118.5	35.0	0.5	0.5
04-001-8928	Cu ₂ V ₂ O ₇	monoclinic	A2/a(15)	10.09	8.01	7.69	90.0	110.3	90.0	582.6	36.4	0.5	0.5
00-059-0012	Cu ₂ V ₂ O ₇	triclinic	P-1(2)	5.83	9.36	5.08	97.1	97.4	99.9	268.2	33.5	0.5	0.5
04-014-0715	Cu ₂ V ₂ O ₇	orthorhombic	Fdd2(43)	8.41	20.68	6.45	90.0	90.0	90.0	1121.6	35.0	0.5	0.5
04-012-8366	Cu ₂ V ₂ O ₇	orthorhombic	Fdd2(43)	8.38	20.65	6.44	90.0	90.0	90.0	1114.9	34.8	0.5	0.5
04-012-0620	Cu ₂ V ₂ O ₇	monoclinic	A2/a(15)	10.11	8.21	7.33	90.0	110.5	90.0	569.3	35.6	0.5	0.5
01-078-2581	Cu ₂ V ₂ O ₇	triclinic	P1(1)	5.55	10.09	5.55	104.0	92.3	104.0	291.0	36.4	0.5	0.5
01-078-2580	Cu ₂ V ₂ O ₇	triclinic	P1(1)	5.62	10.18	5.62	103.6	91.5	103.6	302.8	37.8	0.5	0.5
01-076-2820	Cu ₂ V ₂ O ₇	monoclinic	A2/a(15)	10.11	8.03	7.69	90.0	110.3	90.0	585.4	36.6	0.5	0.5
04-010-7238	CaCuV ₂ O ₇	monoclinic	P2/a(13)	10.19	8.85	10.01	90.0	91.0	90.0	902.1	37.6	0.5	0.25

Table S1, related to “Structural characterization” section. List of phases with relevant crystallographic parameters used to determine volume per cation in several copper vanadate phases as well as CaCuV₂O₇.